Control of Humanoid Hopping Based on a SLIP Model

Patrick M. Wensing and David E. Orin

Abstract Humanoid robots are poised to play an ever-increasing role in society over the coming decades. The structural similarity of these robots to humans makes them natural candidates for applications such as elder care or search and rescue in spaces designed for human occupancy. These robots currently, however, do not have the capability for fast dynamic movements which may be required to quickly recover balance or to traverse challenging terrains. Control of a basic dynamic movement, hopping, is studied here through simulation experiments on a 26 degree of freedom humanoid model. Center of mass trajectories are planned with a spring-loaded inverted pendulum (SLIP) model and are tracked with a task-space controller. Unauthored arm movements emerge from the task-space approach to produce continuous dynamic hopping at 1.5 m/s.

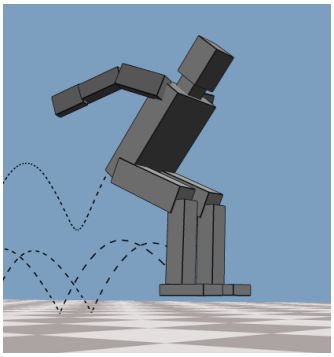

Fig. 1 A combination of SLIP model planning and task-space control allows a continuous dynamic hop to be controlled at real-time rates. The structure of the Task-Space Controller allows unauthored arm action to emerge which prevents extra torso pitching during leg thrust and during positioning of the feet in flight.

Patrick M. Wensing, e-mail: wensing.2@osu.edu
David E. Orin, e-mail: orin.1@osu.edu
The Ohio State University
Dept. of Electrical and Computer Engineering
Columbus, OH 43210

1 Introduction

With the abundance of promising recent work in humanoid robots, these systems are becoming ever closer to operating alongside humans in the home and in the workplace. Mechanical improvements to many of the state-of-the-art humanoids [5, 9, 16, 17] are continually occurring to push the potential applications that they may provide. Aside from mechanical improvements, control of these systems continues to advance as well, for instance, providing intuitive human to robot interactions [1], stable locomotion over mildly uneven terrain [14], and balance recovery from environmental disturbances [3].

Despite these efforts, humanoid robots still have little capability for fast dynamic movements, such as hopping or jumping. These types of movements require coordinated interactions between many degrees of freedom in order to manage the rapid interchanges of kinetic and potential energies throughout stages of stance and flight. Stable performance of these movements is further complicated by short periods of stance, during which large ground forces on the system must be managed within their frictional and unidirectional limits to provide corrective interactions.

As a basic dynamic movement, hopping provides a platform to evaluate control approaches for dynamic motion without the need to address the more complex limb phasings found in derivative movements such as running. Future humanoids operating in challenging environments will require aggressive movements such as a hop to clear obstacles or to traverse areas with widely separated footholds. Hop control has been explored previously in bipeds, where specialized compliant actuators [7] were used to store and return energy to the system during stance. Here, instead, compliant dynamics are mimicked in the humanoid through the use of a physics-based spring-loaded inverted pendulum (SLIP) model to generate reference dynamics for the humanoid center of mass (CoM). This approach enables continuous forward hopping, and manages joint coordination through the use of a task-space controller to select joint torques. Results are shown for full 3D hopping in simulation with a 26 degree of freedom (DoF) humanoid. A snapshot of this model mid-flight is shown in Fig. 1. The fluid resultant hopping motion features arm swing during stance and flight as a natural coordination strategy from the task-space control approach, and emerges without manual authoring.

The remainder of this paper is laid out as follows. Notation to describe the dynamics of the humanoid model and the SLIP template are developed briefly in Section 2. Section 3 presents the Task-Space Controller at a high-level and describes the generation of SLIP-based CoM reference trajectories. Results are presented in Section 4 with a summary provided in Section 5.

2 Simulation and Template Models

The humanoid shown in Fig. 1 is a 26-DoF system that is modeled after a 6 foot (1.83 m), 160 pound (72.6 kg) male. Further details on the model are given

in [18]. The configuration of the system can be described by $\boldsymbol{q} = [\ \boldsymbol{q}_b^T\ \ \boldsymbol{q}_a^T\ ]^T$, where $\boldsymbol{q}_b \in SE(3)$ is the unactuated position and orientation of the torso (referred to as the floating base) and $\boldsymbol{q}_a$ denotes the configuration of the actuated joints. The joint rate and acceleration vectors, $\dot{\boldsymbol{q}} \in \mathbb{R}^{26}$ and $\ddot{\boldsymbol{q}} \in \mathbb{R}^{26}$, are partitioned similarly. The standard dynamic equations of motion are:

$$\boldsymbol{H}(\boldsymbol{q})\ddot{\boldsymbol{q}} + \boldsymbol{C}(\boldsymbol{q},\dot{\boldsymbol{q}})\dot{\boldsymbol{q}} + \boldsymbol{G}(\boldsymbol{q}) = \boldsymbol{S}_a^T\boldsymbol{\tau} + \boldsymbol{J}_s(\boldsymbol{q})^T\boldsymbol{F}_s \tag{1}$$

where $\boldsymbol{H}$, $\boldsymbol{C}\dot{\boldsymbol{q}}$, and $\boldsymbol{G}$ are the familiar mass matrix, velocity product terms, and gravitational terms, respectively. Here $\boldsymbol{F}_s$ collects ground reaction forces (GRFs) for appendages in support, and $\boldsymbol{J}_s$ is a combined support Jacobian. The matrix $\boldsymbol{S}_a = [\mathbf{0}_{20\times 6}\ \ \mathbf{1}_{20\times 20}]$ is a selection matrix for the actuated joints and $\boldsymbol{\tau} \in \mathbb{R}^{20}$ is the joint torque vector. The full 3D dynamics of the humanoid are simulated with the DynaMechs [13] simulation package. This simulator employs a penalty-based contact model which includes compliance and damping in the normal and tangential directions at each planar contact point. No force feedback is provided to the controller.

To generate dynamic hopping, the approach presented in Section 3 will seek to mimic the CoM dynamics described by a SLIP model. This template model for locomotion, shown in Fig. 2, has been shown to describe the CoM dynamics incredibly well for high-speed forward locomotion in a wide array of insects and animals [2, 4, 8]. Species as diverse as crabs to kangaroos bounce in a dynamically similar fashion at high-speeds, and demonstrate similar effective leg stiffnesses relative to their size and weight [2]. In biological systems, the selection of an effectively compliant gait at high speeds instead of a stiff legged gait (which is employed at lower speeds) is due in part to energetic savings that are enabled by the passive compliance of muscles, tendons, and ligaments [4]. Although we assume no joint compliance for the humanoid model used here, it is envisioned that the addition of passive and variable compliance will continue to be an active area of actuation research [6, 10], enabling future humanoids to perform these types of movements with efficiency and power.

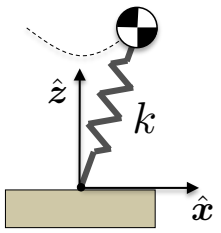

Fig. 2 SLIP stance model for forward locomotion. The position is given relative to an anchor location as (x,z). The model includes a Hookean leg spring with spring constant k. During flight, a ballistic model is assumed for the point mass.

The SLIP model assumes a linear leg spring during stance, with a rest length equal to the touchdown length of the spring. Stance terminates when the leg spring again reaches its rest length, and is followed by ballistic CoM dynamics in flight.

This point-mass model implicitly assumes massless legs that can be arbitrarily repositioned in flight for preparation of the upcoming touchdown.

3 Prioritized Task-Space Control

Task-space (also called operational-space) control provides a convenient framework to allow for control of the salient characteristics of a behavior or movement, without requiring large amounts of motion detail in the high-dimensional configuration space of the humanoid. For instance, natural task spaces such as the CoM and configurations of the feet can be used to generate dynamic walking [12] with minimal required hand authoring. The role of task-space control within the control system used here is shown in Fig. 3. Roughly, the task-space control problem is to select joint torques to reproduce some commanded task dynamics as closely as possible. While task-space control for a manipulator is a well studied problem, the underactuation of a humanoid in flight and stance introduces additional constraints on the solution to the problem. In this work, a state machine (consisting simply of flight and stance states) is used to inform the Task-Space Controller of these constraints, and to manage tracking of the tasks (CoM, feet, posture, etc.).

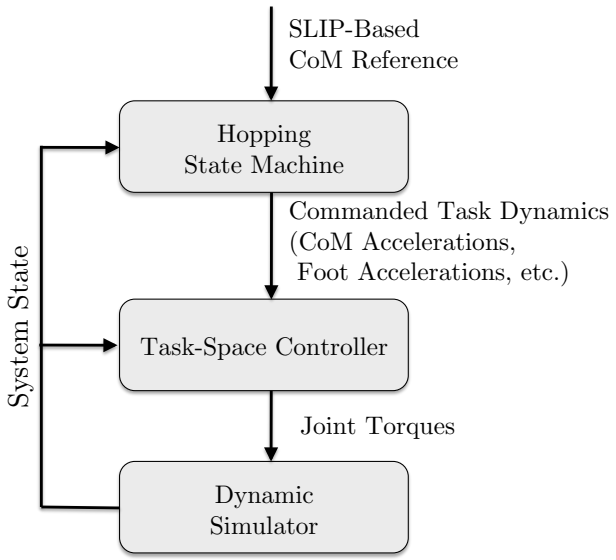

Fig. 3 Overall system block diagram. SLIP-based reference trajectories and hand authored foot trajectories are tracked by the Task-Space Controller. The Hopping State Machine monitors if the system is in flight or stance, and turns off CoM control during flight.

In our recent work [18] we proposed a conic-optimization-based solution to the task-space control problem that uses numerical optimization software to select physically feasible contact forces and joint torques. Roughly, the optimization-based approach enacts task-space control while simultaneously ensuring that the classic force distribution problem (FDP) [11] remains feasible to generate the task dynamics with forces under the feet. To ensure solvability of the FDP, the contact wrench acting on each of the N_S support feet is broken up into forces $\boldsymbol{f}_{s_{ij}} \in \mathbb{R}^3$ which act at each of the N_{P_i} contact vertices for foot i. Then, given a commanded task acceleration $\dot{\boldsymbol{v}}_{t,c}$, an optimization problem described by (2)-(4) can be solved to select ground forces, joint torques, and joint accelerations that are consistent with the system dynamics.

$$\min_{\ddot{\boldsymbol{q}},\tau,\boldsymbol{f}_{s_{ij}}} \quad \frac{1}{2}||\boldsymbol{J}_t\,\ddot{\boldsymbol{q}} + \dot{\boldsymbol{J}}_t\,\dot{\boldsymbol{q}} - \dot{\boldsymbol{v}}_{t,c}||^2 \tag{2}$$

$$\text{subject to } \boldsymbol{H}\,\ddot{\boldsymbol{q}} + \boldsymbol{C}\,\dot{\boldsymbol{q}} + \boldsymbol{G} = \boldsymbol{S}_a^T\,\tau + \sum_{i=1}^{N_S}\sum_{j=1}^{N_{P_i}} \boldsymbol{J}_{s_{ij}}^T \boldsymbol{f}_{s_{ij}} \tag{3}$$

$$\boldsymbol{f}_{s_{ij}} \in \mathscr{C}_i \qquad \forall\, i \in \{1,\ldots,N_S\},\, j \in \{1,\ldots,N_{P_i}\}. \tag{4}$$

Here $\boldsymbol{J}_t$ is a task Jacobian, $\boldsymbol{J}_{s_{ij}}$ is a Jacobian for contact vertex j of foot i, and $\mathscr{C}_i$ is a friction cone for foot i. $\boldsymbol{J}_t$ may be a Jacobian for a stack of tasks and may include, for instance, foot and CoM Jacobians within its rows. In this optimization, (2) enforces optimal tracking of the task dynamics, while (3) and (4) ensure that the the optimal task dynamics are physically realizable.

If a strict hierarchy of importance exists amongst the tasks, then a Prioritized Task-Space Control (PTSC) problem exists. The optimization problem above can be solved first to optimize tracking of the highest-priority task alone, and then subsequently to optimize tracking of the lower-priority tasks. These subsequent optimizations require additional constraints to be added to the problem as described in [18]. This formulation can also be used to regulate angular momentum, as described in [18], even though angular momentum is not amenable to a task Jacobian.

3.1 SLIP-Based CoM Reference Trajectories

SLIP-based CoM reference trajectories are used to generate the commanded CoM accelerations. First, a periodic trajectory of the SLIP model, through stance and flight, is found off-line. This off-line process tunes the SLIP touchdown angle, maximum CoM height during flight, and effective leg stiffness to obtain a periodic gait with user-specified stance and flight times. An example periodic trajectory is shown in Fig. 4. We note that choosing too high of an effective leg stiffness causes the system to slow down from one step to the next, while too low of an effective leg stiffness causes the system to speed up. This is shown in Fig. 5 for a variation of 30 percent above and below the stiffness for periodic locomotion. All cases shown use the touchdown angle and top-of-flight height shown in Fig. 4.

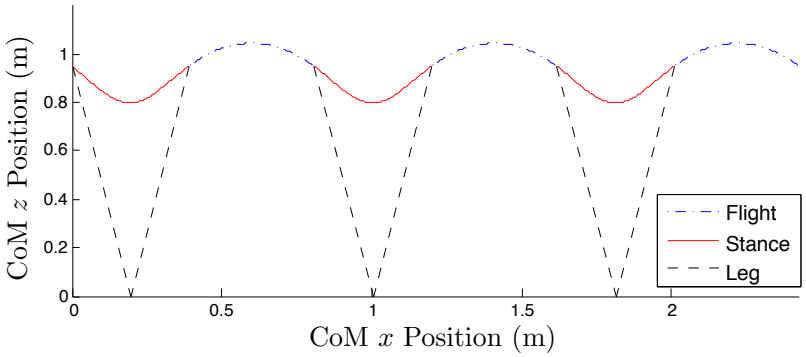

Fig. 4 SLIP-based CoM reference trajectory for 1.5 m/s forward hopping. Touchdown and liftoff angles are symmetric, which holds for every 1 step periodic trajectory of the SLIP model.

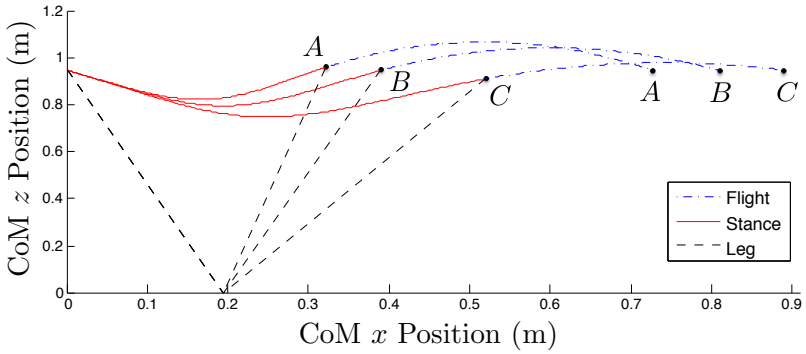

Fig. 5 Comparison of CoM trajectories for varying leg stiffness. Trajectory B uses the leg stiffness found to generate periodic CoM motion, while A and C employ stiffnesses that are 30% greater and 30% less, respectively.

The periodic SLIP trajectory is followed on-line through a simple PD control law to select the commanded CoM acceleration (which composes three of the components of $\dot{\boldsymbol{v}}_{t,c}$). With the CoM position given as $\boldsymbol{p}_G$, the commanded acceleration $\ddot{\boldsymbol{p}}_{G,c}$ is specified as

$$\ddot{\boldsymbol{p}}_{G,c} = \ddot{\boldsymbol{p}}_{G,d} + \boldsymbol{K}_D(\dot{\boldsymbol{p}}_{G,d} - \dot{\boldsymbol{p}}_G) + \boldsymbol{K}_P(\boldsymbol{p}_{G,d} - \boldsymbol{p}_G) \tag{5}$$

where $(\boldsymbol{p}_{G,d}, \dot{\boldsymbol{p}}_{G,d}, \ddot{\boldsymbol{p}}_{G,d})$ are the desired values from the SLIP based trajectory. The lateral position of the CoM is commanded to remain at a fixed initial position. We note that it is possible to employ a series of PD setpoints, as in [18] to achieve a standing jump. However, continuous hopping requires more careful design of CoM trajectories. The biological grounding of the SLIP model makes it a natural choice to generate these trajectories, and does so with little required hand authoring.

3.2 State-Based Control Summary

Periods of stance and flight require different task-space dynamics to be controlled. During periods of stance, CoM control is active, and the feet are constrained to not accelerate (linearly or rotationally). Feet are chosen as a first priority (within PTSC), and the CoM as a second priority. Given its many DoFs, the system is redundant to achieve these tasks. Thus, we add additional pose tasks for each joint to promote the return to a natural posture [18]. In addition, the net system angular momentum (as expressed at the CoM) is regulated to zero in the forward and vertical directions to promote balance [15]. These additional tasks more than exhaust the redundancy available after tracking the CoM and feet. As a result, task-weightings are placed on each degree of freedom when evaluating the error norm in (2). For instance, it is important to maintain upright torso posture during any movement, yet the specific motion of the arms is largely unimportant. As a result, task weightings assigned to torso posture are approximately seven times higher than those on the arm DoFs.

In flight, the CoM follows a ballistic trajectory and is not controlled, while the feet remain a high priority in preparation for the upcoming touchdown. Foot trajectories are manually designed relative to the CoM and are commanded to accelerate with PD laws similar to (5). Due to conservation of angular momentum in flight, the configuration of the system at landing is sensitive to flight foot trajectories. That is, any change in angular momentum of the legs during flight must be countered by opposite angular momentum changes in the upper body. The practical implication of this fact is that leg transfer trajectories that are performed with the feet closer to the body result in less pitched-forward torso disturbance at touchdown.

4 Results

The control approach described enables continuous forward hopping at 1.5 m/s. Snapshots from this motion in simulation[1] are shown in Fig. 6. Fig. 7 shows the close tracking of the SLIP reference velocities despite impact disturbances that de-

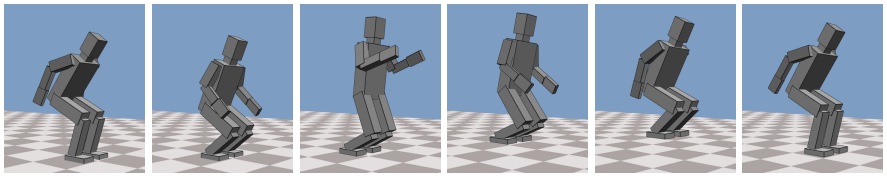

Fig. 6 Simulation snapshots for periodic hopping at 1.5 m/s. Arm swing motions are a natural coordination that emerge due to the reduced task weighting of the arm joints in the PTSC.

[1] A video of this hopping motion is provided at
`http://go.osu.edu/Wensing_Orin_Waldron2013`

grade the tracking at touchdown. We note that the gait shown here uses a nondimensional leg stiffness [2] of 19.6, which normalizes the effective leg stiffness for systems of different size and weight. This effective leg stiffness is within one standard deviation of average stiffnesses observed in biological hoppers such as kangaroos [2].

We note that the arm swing trajectories that emerge as a coordination strategy from the PTSC allow for tighter regulation of the torso posture as shown in Fig. 8. Arms swing backwards during flight to offset the change in angular momentum of the legs. Without their influence, the torso pitches forward additionally prior to touchdown. While not shown here, the removal of foot lift during flight foot positioning has similar negative influence on the torso during flight.

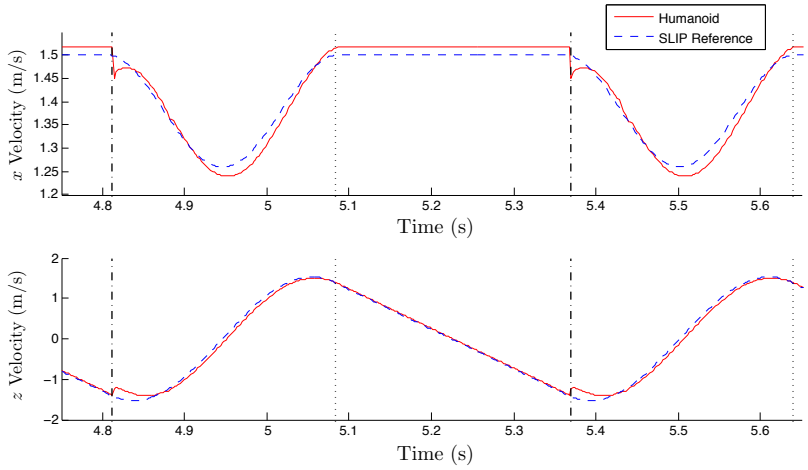

Fig. 7 CoM velocity tracking for 1.5 m/s forward hopping. Vertical bars indicate transitions between stance and flight states.

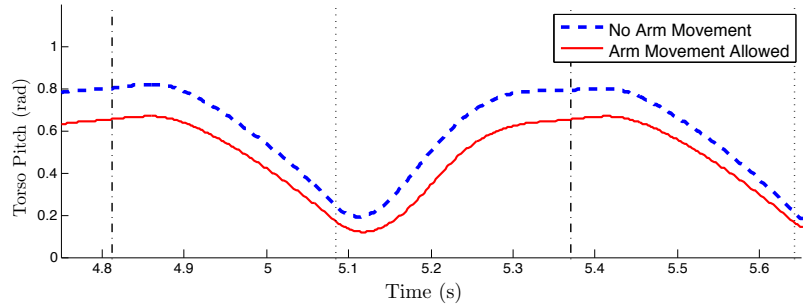

Fig. 8 The flexibility to allow arm movement with PTSC allows for tighter regulation of the torso pitch during stance and flight. The torso pose controller here employs a zero setpoint of nominally upright.

By varying the leg stiffness and other SLIP template characteristics, other more dynamic (and less biologically grounded) hopping gaits may be generated. As shown in the video accompaniment to this work, gaits with additional foot clearance can be generated through specification of periodic CoM trajectories with lower effective leg stiffness. A second gait showcased in the accompanying video employs an effective leg stiffness that is approximately one-half of that required for the gait in Fig. 4. A larger touchdown angle, coupled with this decreased stiffness allows for more vertical CoM variation in stance, and provides longer flight times with higher maximum heights.

5 Summary

The spring-loaded inverted pendulum model has been shown to be an enabling template for the generation of continuous dynamic hopping. The ability of the SLIP model to capture the salient dynamics of a periodic hop enables the control approach here to be applied with little more than the authoring of a set of foot trajectories. A task-space control approach, which enforces feasibility of the force distribution problem at each instant, effectively manages system balance through prioritization of balance tasks and weighted pose tracking.

While the approach here has shown positive results for hopping, the methods presented should enable control of other dynamic movements with significant contributions from out-of-plane effects. Simple template models of dynamic locomotion that capture out-of-plane effects, such as the 3D-SLIP model, will be studied in future work to enable a richer set of dynamic movement capabilities for humanoid robots.

6 Acknowledgments

This paper is dedicated to Professor Ken Waldron, who was a great inspiration to our work in legged locomotion at Ohio State. His leadership in several research projects sponsored by DARPA and NSF has had a significant impact on our program in robotics.

This work was supported by a National Science Foundation Graduate Research Fellowship to Patrick Wensing, and by Grant No. CNS-0960061 from the NSF with a subaward to The Ohio State University.

References

1. Arumbakkam, A., Yoshikawa, T., Dariush, B., Fujimura, K.: A multi-modal architecture for human robot communication. In: IEEE-RAS Int. Conf. on Humanoid Robots, pp. 639–646 (2010)
2. Blickhan, R., Full, R.: Similarity in multilegged locomotion: Bouncing like a monopode. Journal of Comparative Physiology A **173**, 509–517 (1993)
3. Cho, B.K., Park, S.S., Oh, J.H.: Stabilization of a hopping humanoid robot for a push. In: IEEE-RAS Int. Conf. on Humanoid Robots, pp. 60–65 (2010)
4. Farley, C.T., Glasheen, J., McMahon, T.A.: Running springs: speed and animal size. Journal of Experimental Biology **185**(1), 71–86 (1993)
5. Gouaillier, D., Collette, C., Kilner, C.: Omni-directional closed-loop walk for NAO. In: IEEE-RAS Int. Conf. on Humanoid Robots, pp. 448–454 (2010)
6. Grebenstein, M., Albu-Schaffer, A., Bahls, T., Chalon, M., Eiberger, O., Friedl, W., Gruber, R., Haddadin, S., Hagn, U., Haslinger, R., Hoppner, H., Jorg, S., Nickl, M., Nothhelfer, A., Petit, F., Reill, J., Seitz, N., Wimbock, T., Wolf, S., Wusthoff, T., Hirzinger, G.: The DLR hand arm system. In: IEEE Int. Conf. on Robotics and Automation, pp. 3175–3182 (2011)
7. Hester, M., Wensing, P.M., Schmiedeler, J.P., Orin, D.E.: Fuzzy control of vertical jumping with a planar biped. In: Proc. of the ASME Int. Design Engineering Technical Conferences, (Montreal, Canada), pp. DETC2010–28857:1–9 (2010)
8. Holmes, P., Full, R.J., Koditschek, D., Guckenheimer, J.: The dynamics of legged locomotion: Models, analyses, and challenges. SIAM Rev. **48**(2), 207–304 (2006)
9. Kaneko, K., Kanehiro, F., Morisawa, M., Akachi, K., Miyamori, G., Hayashi, A., Kanehira, N.: Humanoid robot HRP-4 - humanoid robotics platform with lightweight and slim body. In: IEEE/RSJ Int. Conf. on Intelligent Robots and Systems, pp. 4400–4407 (2011)
10. Knox, B.T., Schmiedeler, J.P.: A unidirectional series-elastic actuator design using a spiral torsion spring. Journal of Mechanical Design **131**(12), 125001:1–5 (2009)
11. Kumar, V., Waldron, K.: Force distribution in closed kinematic chains. IEEE Journal of Robotics and Automation **4**(6), 657–664 (1988)
12. de Lasa, M., Mordatch, I., Hertzmann, A.: Feature-based locomotion controllers. In: ACM SIGGRAPH 2010 papers, vol. 29, pp. 131:1–10. ACM, New York, NY, USA (2010)
13. McMillan, S., Orin, D.E., McGhee, R.B.: DynaMechs: an object oriented software package for efficient dynamic simulation of underwater robotic vehicles. In: Underwater Robotic Vehicles: Design and Control, pp. 73–98. TSI Press, Albuquerque, NM (1995)
14. Morisawa, M., Kanehiro, F., Kaneko, K., Kajita, S., Yokoi, K.: Reactive biped walking control for a collision of a swinging foot on uneven terrain. In: IEEE-RAS Int. Conf. on Humanoid Robots, pp. 768–773 (2011)
15. Orin, D.E., Goswami, A.: Centroidal momentum matrix of a humanoid robot: Structure and properties. In: IEEE/RSJ Int. Conf. on Intelligent Robots and Systems, pp. 653–659 (2008)
16. Park, I.W., Kim, J.Y., Lee, J., Oh, J.H.: Mechanical design of humanoid robot platform KHR-3 (KAIST humanoid robot 3: HUBO). In: IEEE-RAS Int. Conf. on Humanoid Robots, pp. 321–326 (2005)
17. Sakagami, Y., Watanabe, R., Aoyama, C., Matsunaga, S., Higaki, N., Fujimura, K.: The intelligent ASIMO: system overview and integration. In: IEEE/RSJ Int. Conf. on Intelligent Robots and Systems, vol. 3, pp. 2478–2483 (2002)
18. Wensing, P.M., Orin, D.E.: Generation of dynamic humanoid behaviors through task-space control with conic optimization (2013), to appear In: Proc. of the IEEE Int. Conf. on Robotics and Automation